Applications of Ultrafast Lasers for Optical Measurements in Combusting Flows*

James R. Gord,[1] Terrence R. Meyer,[2] and Sukesh Roy[1]

[1]Air Force Research Laboratory, Propulsion Directorate, Wright-Patterson Air Force Base, Ohio 45433; email: james.gord@wpafb.af.mil, sroy@woh.rr.com

[2]Mechanical Engineering Department, Iowa State University, Ames, Iowa 50011; email: trm@iastate.edu

Annu. Rev. Anal. Chem. 2008. 1:663–87

First published online as a Review in Advance on March 18, 2008

The *Annual Review of Analytical Chemistry* is online at anchem.annualreviews.org

This article's doi:
10.1146/annurev.anchem.1.031207.112957

1936-1327/08/0719-0663$20.00

*Erratum

Key Words

combustion diagnostics, laser-induced fluorescence, pump/probe, ballistic imaging, coherent anti-Stokes Raman scattering, wave mixing

Abstract

Optical measurement techniques are powerful tools for the detailed study of combustion chemistry and physics. Although traditional combustion diagnostics based on continuous-wave and nanosecond-pulsed lasers continue to dominate fundamental combustion studies and applications in reacting flows, revolutionary advances in the science and engineering of ultrafast (picosecond- and femtosecond-pulsed) lasers are driving the enhancement of existing diagnostic techniques and enabling the development of new measurement approaches. The ultrashort pulses afforded by these new laser systems provide unprecedented temporal resolution for studies of chemical kinetics and dynamics, freedom from collisional-quenching effects, and tremendous peak powers for broad spectral coverage and nonlinear signal generation. The high pulse-repetition rates of ultrafast oscillators and amplifiers allow previously unachievable data-acquisition bandwidths for the study of turbulence and combustion instabilities. We review applications of ultrafast lasers for optical measurements in combusting flows and sprays, emphasizing recent achievements and future opportunities.

*This PDF amended on (25 Jun. 2008): See explanation at http://arjournals.annualreviews.org/errata/anchem

1. INTRODUCTION

CARS: coherent anti-Stokes Raman scattering

RFWM: resonant four-wave mixing

Propulsion systems represent a substantial fraction of the cost, weight, and complexity of aircraft and spacecraft. The vast majority of these propulsion systems are powered through fuel combustion; therefore, the detailed study of fundamental combustion phenomena has emerged as a highly relevant and important field of endeavor. Today's combustion scientists and engineers devote much of their work to improving propulsion-system performance while simultaneously reducing pollutant emissions. Increasing the affordability, maintainability, and reliability of these critical propulsion systems is a major driver of activity as well.

Although our efforts in the Combustion and Laser Diagnostics Research Complex at Wright-Patterson Air Force Base are focused primarily on combustion phenomena associated with air-breathing and rocket propulsion, a host of other applications drive advances in combustion science as well. These include internal-combustion engines, land- and sea-based power generation, industrial processing, combustion-based synthesis, waste incineration, and fire safety, for example. Clean, efficient combustion technologies and alternative fuels (e.g., Fischer-Tropsch fuels and biofuels) are critical for meeting current and future energy demands while reducing our dependence on fossil fuels and minimizing such environmental impacts as smog, particulates, acid rain, greenhouse gases, and global warming.

Advanced measurement techniques that exploit lasers and optics have become well-established tools for characterizing combusting flows (1–4). Such noninvasive measurement approaches are often ideally suited for visualizing complex reacting flows and quantifying key chemical-species concentrations, temperature, and fluid-dynamic parameters. The fundamental information these techniques provide is essential for achieving a detailed understanding of the chemistry and physics of combustion processes.

Many successful optical measurements achieved to date in combusting flows have been based on the use of conventional continuous-wave and nanosecond-pulsed laser systems, including Q-switched Nd:YAG lasers, excimer lasers, and associated YAG- and excimer-pumped dye lasers. These systems have been the workhorses in most experiments involving such optical measurement techniques as planar laser-induced fluorescence, particle-image velocimetry, laser-induced incandescence, coherent anti-Stokes Raman scattering (CARS) spectroscopy, and resonant four-wave mixing (RFWM). These laser systems afford high pulse energies required for sheet lighting in planar techniques and for nonlinear interactions such as those in CARS and RFWM. They also provide the relatively narrow spectral bandwidths required for spectroscopic studies of key gas-phase combustion species (e.g., OH, CH, NO, and CO).

Although the impact of continuous-wave and nanosecond-pulsed lasers systems on the modern science of combustion measurements is undeniable, continuing revolutionary advances in the science and engineering of ultrafast lasers (i.e., picosecond- and femtosecond-pulsed lasers) (5–8) have enhanced the capabilities and utility of existing combustion-diagnostic techniques while enabling the development and application of new measurement methodologies previously unachievable. Early

practitioners pioneered ultrafast combustion measurements based on modelocked argon-ion and Nd:YAG lasers with synchronously pumped dye lasers, but the advent of modelocked titanium:sapphire (Ti:sapphire) oscillators and amplifier systems based on regenerative and multipass configurations and chirped-pulse amplification has changed the landscape dramatically, accelerating the development and application of new ultrafast laser–based combustion diagnostics.

PS: polarization spectroscopy

Regardless of the architecture, two key features of ultrafast lasers are responsible for the tremendous utility they afford for combustion measurements: ultrashort pulses and high pulse-repetition rates. Myriad beneficial characteristics stem from the ultrashort picosecond and femtosecond pulses delivered by modern ultrafast laser systems. These advantages of ultrashort pulses are realized in terms of the time resolution achievable and the temporal duration of the optical combustion measurements. In addition, ultrashort pulses enable tremendous instantaneous power from laser systems of moderate to low average power.

The time resolution afforded by ultrafast laser systems has been exploited to study the kinetics and dynamics of combustion chemistry and energy-transfer processes. Investigators have used separation in time of various pump and probe pulses to discriminate against nonresonant background signals, enhancing measurement sensitivity and selectivity and enabling the determination of key minor-species concentrations. Because of the ultrashort duration of some of these measurements, signals can be acquired that are largely free of collisional and pressure effects. This key feature of ultrafast combustion measurements addresses one of the major limitations of conventional nanosecond-pulsed diagnostics, and it enables quantitative measurements of parameters such as number densities and temperature in high-pressure, turbulent flames characteristic of most practical combustion devices. In these systems the collisional-quenching environment is typically highly inhomogeneous and rapidly changing in both space and time.

The instantaneous power from these ultrafast laser systems has been exploited to drive many desirable nonlinear phenomena. Researchers have utilized such nonlinearities to expand the spectral coverage available from these laser systems and to achieve various novel higher-order signals based on multiple-wave mixing. Amplified Ti:sapphire-based systems can deliver usable radiation throughout an impressive spectral region across the ultraviolet (UV), visible, and infrared. Through continuing advances involving laser-matter interactions and higher-order harmonic generation, extreme UV radiation and X-rays can be produced for diagnostic applications. At the opposite end of the spectrum, terahertz radiation has been generated using ultrafast lasers and applied to combustion measurements. Nonlinear signal generation in combusting flows has been explored with ultrafast lasers and wave-mixing techniques that include polarization spectroscopy (PS), CARS, and RFWM (described in detail below).

Many ultrafast laser systems deliver very high pulse-repetition rates. Modelocked oscillators feature repetition rates of the order ~100 GHz, and commercially available amplifiers deliver pulses at rates up to 1–300 kHz. Fluctuation timescales of the order 1–100 μs characterize the high-pressure, turbulent combustion environments found in most practical devices. Although conventional 10-Hz, nanosecond-pulsed laser

LIF: laser-induced fluorescence

systems can be used to study these turbulent combustion environments, they provide only probability density functions for combustion parameters and cannot capture time correlations describing fluctuating turbulent combustion. Investigators have used measurements based on high-repetition-rate, ultrafast laser systems, conversely, to capture probability density functions, as well as time series, time correlations, and power spectral densities (PSDs) describing the frequency content of turbulent phenomena of interest.

In the sections below, we review the advantages of ultrafast laser systems for optical combustion measurements with special emphasis on applications involving ultrafast laser-induced fluorescence (LIF), linear pump/probe techniques, time-gated ballistic imaging, ultrafast CARS spectroscopy, and resonant and Raman PS and wave mixing. Advances stemming from the ultrashort pulses and high pulse-repetition rates provided by ultrafast lasers are evident throughout these applications.

2. ULTRAFAST LASER-INDUCED FLUORESCENCE

LIF has been used extensively for measurements of minor-species concentrations and gas temperature in reacting and nonreacting flows (1–4). Measurements of minor species are important for understanding flame chemistry and validating models of ignition, heat release, flame propagation, pollutant formation, and flame extinction. The availability of picosecond lasers for time-resolved LIF has played a critical role in the study of energy-transfer processes, in extending LIF measurements to the deep UV, and in improving the quantitative nature of LIF in unknown quenching environments.

The quantitative interpretation of LIF signals requires detailed knowledge of molecular energy-transfer processes such as electronic quenching, rotational energy transfer (RET), and vibrational energy transfer. One can easily investigate these processes, which compete with the radiative decay of the excited state, at low pressures using nanosecond lasers (9). At atmospheric pressure, however, transfer rates must be measured with picosecond resolution given gas collision rates that yield fluorescence lifetimes of the order 1 ns.

A typical setup for OH LIF comprises a chirped-pulse amplified Ti:sapphire laser system (1.5-ps pulse width, 0.5 mJ per pulse) that is frequency tripled to the UV near 284 nm (1-ps pulse width, 20 μJ per pulse) (10). Other investigators have used a Raman-excimer laser in combination with stimulated Brillouin scattering (11), passive and active modelocking in combination with stimulated Brillouin scattering (12), or regenerative amplification with or without a distributed-feedback dye laser (13, 14) to achieve ∼100-ps pulses with sufficient spectral resolution (of the order 0.5 cm^{-1} at atmospheric pressure) to isolate individual rotational transitions. Another advantage of picosecond lasers is the ability to access species such as H atoms (12), O atoms (15, 16), CO (17), and NO (18) through two-photon excitation. Typical detection schemes include fast photomultiplier tubes, streak cameras, and fast-gated optical imagers for time-resolved studies of collisional quenching, RET, and vibrational energy transfer (9–18).

In addition to fundamental studies of energy-transfer processes for LIF, ultrafast lasers have also been applied for quantitative measurements in flames of practical

interest. In particular, a number of researchers have used fluorescence lifetimes for quantitative measurements of minor-species concentrations in flames in which the temperature and colliding-species concentrations may be unknown. These lifetimes, which are largely dominated by collisional quenching for atmospheric-pressure flames, are typically of the order ~1–3 ns and require the use of a picosecond laser for sufficient time resolution. Application of this approach is particularly important in unsteady, turbulent flames. Studies have been performed for vortex/flame interactions (19) and two-dimensional imaging (20) using picosecond LIF with streak cameras. In turbulent flames, it is also desirable to compute the PSD to analyze the frequency content of number-density fluctuations. To obtain longer time series for PSD measurements of minor species, one can employ a picosecond Ti:sapphire oscillator along with a multichannel photon-counting system for on-the-fly quenching corrections based on fluorescence-lifetime measurements (21, 22). This eliminates uncertainties due to the variation of temperature and colliding-species concentrations in turbulent flames. Time-series measurements have been made for CH (23) and OH (24), as well as OH and temperature (25). **Figure 1** shows a schematic of the optics layout and time-gating approach for the latter, and **Figure 2** shows typical time-resolved OH and temperature measurements in a vortex/flame burner.

Picosecond lasers have been instrumental in improving our understanding of molecular energy-transfer processes in LIF. In addition, picosecond LIF has proven to be useful in turbulent flames in which LIF signals are influenced by local variations in the rate of collisional quenching.

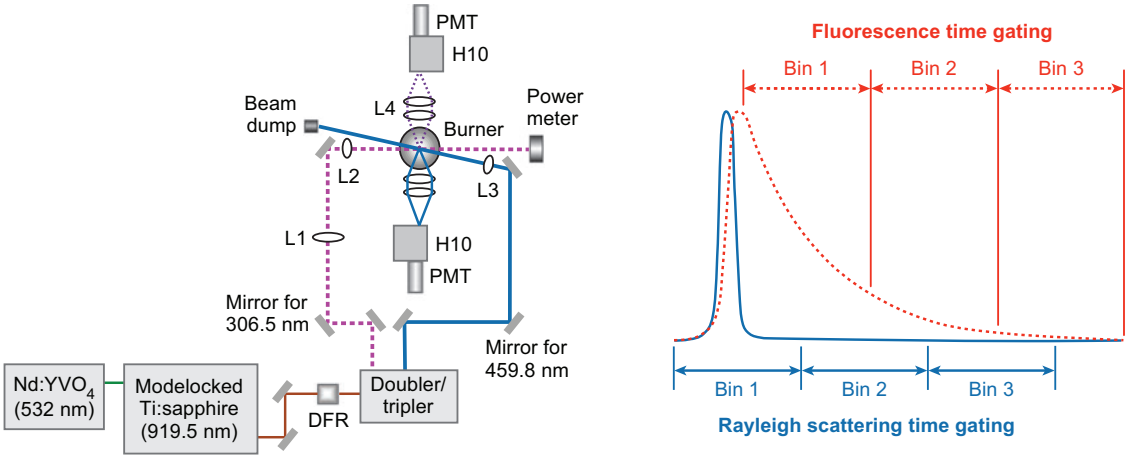

Figure 1

Optical layout (*left panel*) and time-gating diagram (*right panel*) for simultaneous Rayleigh scattering and lifetime-corrected OH laser-induced fluorescence. Bins 1–3 integrate over 3.5-ns bins to detect Rayleigh scattering and resolve fluorescence lifetime assuming single exponential decay. Abbreviations used: DFR, double Fresnel rhomb; H10, 0.1-m monochromator; L1, 1-m lens; L2, 20-cm lens; L3, 20-cm lens; L4, 15-cm lens; PMT, photomultiplier tube. Figure reprinted with permission from Reference 25. Copyright 2007, Optical Society of America.

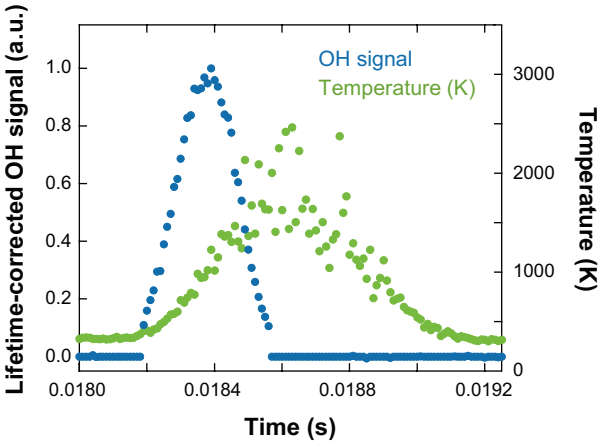

Figure 2

Simultaneous measurements of temperature and lifetime-corrected OH laser-induced fluorescence during vortex/flame interaction.

3. LINEAR PUMP/PROBE TECHNIQUES

A number of groups have developed and applied linear pump/probe techniques to measure absolute number densities of key species as well as temperature in combusting flows. These techniques are linear in the sense that the combustion analyte under study interacts linearly with the pump beam (i.e., a one-photon pump-analyte interaction) and linearly with the probe beam (i.e., a one-photon probe-analyte interaction). Typically in these experiments, the pump beam interacts with the analyte in a linear, one-photon absorption process, transferring some population from the ground electronic state to an excited electronic state, thereby creating a transient hole in the ground-state population and a transient excited-state population. The probe beam subsequently interacts with this transient population distribution through one or more of three processes, based in large part on the spectral characteristics of the probe beam. A probe beam spectrally resonant with ground-state absorption features of the analyte experiences a transient reduction in absorption upon interaction with the pump-modified population distribution. This is manifested as a transient gain in the transmitted intensity of the probe beam. A probe beam spectrally resonant with emission features of the analyte experiences a transient enhancement through stimulated emission upon interaction with the pump-modified population distribution. This is also manifested as a transient gain in the transmitted intensity of the probe beam. A probe beam spectrally resonant with excited-state absorption features of the analyte experiences a transient increase in absorption upon interaction with the pump-modified population distribution. This is manifested as a transient bleach in the transmitted intensity of the probe beam. As the redistribution of population induced by the pump beam relaxes in time, so too do the transient phenomena associated with the probe-beam transmission.

In practice investigators often observe these transient phenomena experimentally by modulating the pump-beam intensity. This modulation is transferred from the pump beam to the analyte population distribution and thereby onto the probe beam. Lock-in detection of the transmitted probe beam reveals the extent of modulation

transfer from the pump beam to the probe beam, and the lock-in signal scales linearly with the analyte concentration. The time delay between the pump and probe beams can be adjusted to explore the temporal characteristics of the population-relaxation dynamics.

ASOPS: asynchronous optical sampling

Lytle and coworkers (26, 27) developed and applied an ingenious scheme for scanning the pump/probe delay and exploring the temporal evolution of the population relaxation using a technique they termed asynchronous optical sampling (ASOPS). In ASOPS, two separate laser oscillators are used—one for the pump beam and one for the probe beam. The optical cavities of the two oscillators are adjusted to slightly different lengths such that the two oscillators operate at slightly different pulse-repetition rates. This difference in pulse-repetition rates is manifested as a repetitive phase walkout between the pump and probe pulses that repeats at Δf, the difference between the two pulse-repetition rates. A no-moving-parts pump/probe delay is achieved without the need for an optomechanical delay line (see **Figure 3**).

The ASOPS technique complements the LIF techniques described in Section 2 above and similar to those techniques can be used to measure absolute number densities and explore the detailed, time-evolving collisional-quenching environments in turbulent combustion through the determination of the population lifetime decay. Fiechtner and coworkers (28–31) applied ASOPS to the measurement of atomic sodium and OH in various laboratory flames. They developed rate-equation models to extract quantitative number densities and collisional-quenching rates from these ASOPS experiments (30, 32).

Fiechtner & Linne (33) pursued a simplified pump/probe arrangement with a fixed pump/probe delay rather than a scanning delay. Although this approach does not reveal the temporal evolution of population relaxation, it can be configured to yield measurements of absolute number densities of key chemical species free from the effects of collisional quenching, provided the fixed pump/probe delay is set such that the probe beam interacts with the pump-modified analyte on a timescale that is short with respect to the collisional timescale. In this fashion, Settersten and coworkers

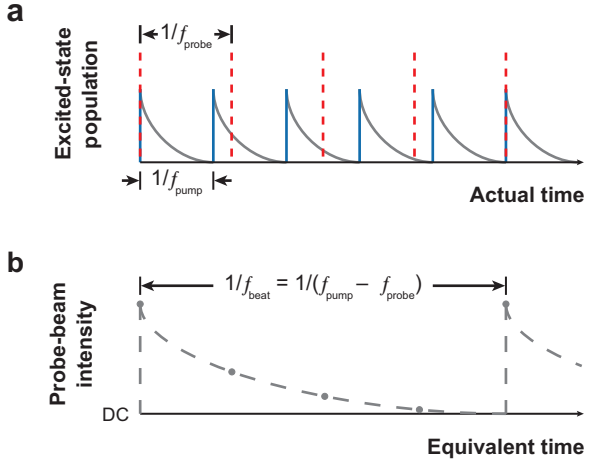

Figure 3

Conceptual asynchronous optical sampling timing diagram depicting (*a*) excited-state population and (*b*) probe-beam intensity upon stimulated emission. Pump pulses are indicated in blue, and probe pulses are indicated in red.

THz-TDS: terahertz time-domain spectroscopy

(34, 35) achieved measurements of potassium and other species in various laboratory flames and modeled the characteristics of the pump/probe signal using rate equations and density-matrix equations (34–37). By forming the pump beam into a laser light sheet and crossing that pump-beam sheet with an upcollimated probe beam in a premixed methane-air flame maintained on a Meeker-type burner, Linne et al. (38) achieved ultrafast linear pump/probe two-dimensional imaging of potassium seeded into the flame.

Advances in ultrafast laser systems have driven tremendous innovations in sensing with terahertz radiation (39). We can also consider terahertz time-domain spectroscopy (THz-TDS) as a linear pump/probe technique, although the pump and probe interactions differ from those discussed above. In the pump/probe experiments described above, the pump and probe beams interact directly with the analyte; however, the pump and probe beams serve different purposes in THz-TDS. In these experiments, the pump beam from a femtosecond-pulsed laser interacts with a target material to generate broadband terahertz radiation, either through photoconduction in a biased semiconductor (e.g., low-temperature-grown GaAs) or through optical rectification (a process described in detail in Reference 39) in a nonlinear medium. When the pulsed terahertz radiation generated in this fashion is transmitted through an absorbing analyte, the spectral and temporal characteristics of the terahertz pulse are modified through linear absorption processes. The probe beam is utilized for time-gated detection of the transmitted terahertz pulse, either through photoconductive or electro-optic sampling. By scanning the pump/probe delay, one can capture the temporal characteristics of the transmitted terahertz pulse, and the Fourier transformation of that pulse yields its frequency-resolved transmission spectrum from which terahertz absorption features of the analyte are determined.

Cheville & Grishchkowsky (40, 41) measured species concentrations and temperature in premixed propane-air flames with THz-TDS techniques based on a traditional optomechanical scanning delay line for variation of the pump/probe delay. Brown et al. (42) adopted the ASOPS scheme described above for H_2O-vapor measurements with a no-moving-parts pump/probe delay. The potential for future applications of THz-TDS in combustion is promising. The terahertz spectral region is rich in absorption features of interest for the quantification of key combustion species (especially H_2O) and temperature. Furthermore, hydrocarbon fuels and carbonaceous soot exhibit little or no absorption in this spectral region, suggesting that THz-TDS should be an ideal technique for measurements in liquid-hydrocarbon-fueled, highly sooting combustion environments such as those characteristic of most practical devices.

4. TIME-GATED BALLISTIC IMAGING

As light propagates through a turbid medium, its direction, polarization, and phase are altered owing to gradients in the index of refraction. Diffuse photons pass through the sample volume with significant multiple scattering events and emerge with a shift in location and direction. This is shown schematically in **Figure 4*a*** and leads to the blurring of internal features within the medium. Snake photons are altered to a

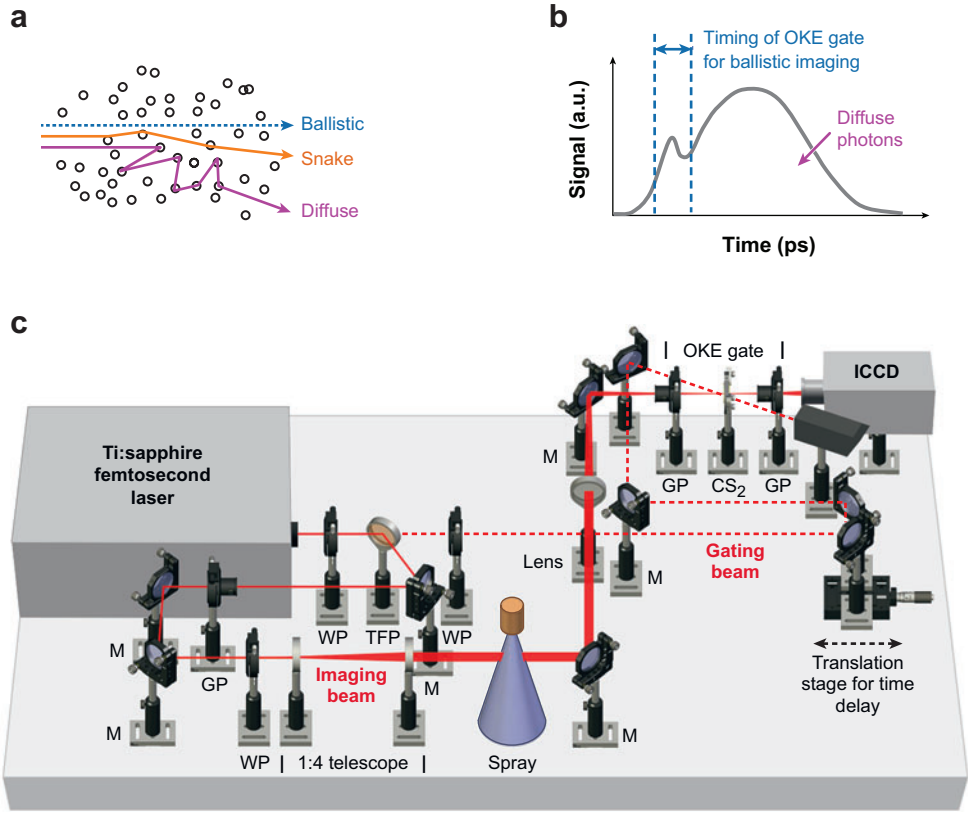

Figure 4

Conceptual picture of (*a*) ballistic, snake, and diffuse photons; (*b*) time trace of signal on detector; and (*c*) optical layout for time-gated ballistic-photon imaging. Abbreviations: GP, Glan polarizer; ICCD, intensified charge-coupled device camera; M, mirror; OKE, optical Kerr effect; TFP, thin film polarizer; WP, half-wave plate.

lesser degree as they propagate with relatively few scattering events, whereas ballistic photons pass through without deviation and maintain their direction of propagation, polarization, and phase.

Interest in utilizing ballistic photons for imaging applications is driven by the possibility that one could use visible and infrared light sources to image turbid media without the need for ionizing radiation or synchrotron sources. The general approach is to separate ballistic or snake photons from diffuse photons using differences in direction, polarization, coherence, or temporal properties of the light passing through the medium. It is possible, for example, to employ a spatial filter to reduce photons that have lost collimation or confocal properties after exiting the sample volume (43, 44). Polarization gating involves the use of an analyzer rather than a spatial filter (45, 46), whereas coherence gating can be accomplished using nonlinear mixing processes (e.g., second-harmonic generation or holography) to discriminate against scattered photons (47–50).

In many cases, spatial filtering and polarization gating may not provide sufficient discrimination against diffuse photons, whereas coherence gating may be too restrictive in that it can eliminate all but the ballistic photons. For unsteady multiphase flows, it is often necessary to use both snake and ballistic photons to have sufficient signal levels for instantaneous two-dimensional imaging of transient mixing processes. One approach, enabled by the availability of ultrafast lasers, is to distinguish photons based on passage time through the turbid medium. A femtosecond laser beam that undergoes significant scattering exits with longer pulse width (order picosecond) because diffuse photons travel a longer path through the sample volume. This longer path is shown schematically in **Figure 4*a*** along with a conceptual view in **Figure 4*b*** of short time gating to discriminate against diffuse photons.

Early work on time-domain photon discrimination demonstrated that one could use picosecond lasers to achieve gate widths on the order of 7–10 ps using an optical Kerr-effect (OKE) time gate consisting of a CS_2 cell placed between a pair of crossed polarizers (51–53). Birefringence with a short relaxation time is induced in the CS_2 upon excitation with an ultrafast laser pulse, allowing light to pass through the crossed polarizers through adjustment of a translation stage to vary the time delay between the imaging and gating beams. Investigators have used this approach for discriminating against diffuse photons in a number of applications (54, 55). With the availability of amplified femtosecond laser systems, it has become possible to achieve time gates as short as 2 ps with high transmission efficiency (56–60).

Figure 4*c* shows an example of the optical setup for time-gated ballistic imaging. The linearly polarized 1 mJ per pulse output of a 1 kHz repetition rate Ti:sapphire amplifier with 80-fs pulse width is split 90% and 10% into gating and imaging beams, respectively, using a wave plate–polarizer combination. The imaging path includes a Glan polarizer, a half-wave plate, and a beam-expanding telescope. After passing through a dense spray, the imaging beam is weakly focused through the OKE gate, then spatially filtered, and relay imaged directly into an intensified charge-coupled device camera. The gating beam passes through a half-wave plate and a mechanical time-delay stage before arriving at the 1-cm-thick, 2.5-cm-diameter CS_2 cell. The induced birefringence across the imaging beam is kept fairly constant within the CS_2 cell because the imaging beam is relatively small (<500-μm diameter) and passes through the centroid of the relatively large gating beam (~6-mm diameter). The transmission efficiency of the OKE gate is ~30% when activated by the 80-fs laser pulse, which is sufficient for signal-to-leakage ratios of ~20:1. This arrangement allows instantaneous two-dimensional imaging of turbid media, in this case a liquid spray. Laser sources with repetition rates as high as 10 kHz with 1 mJ per pulse are now available and will enable ballistic imaging at unprecedented data rates.

This approach has been used for measurements of liquid breakup phenomena in diesel sprays (58), liquid jets in gaseous crossflow (59), and coaxial rocket injectors. **Figure 5** shows an example of coaxial rocket injectors, comparing a rocket spray shadowgram with and without time gating. Internal structures that were previously not visible due to diffuse scattering are revealed with the use of ultrafast time gating. This has implications for the study of liquid jet breakup and gas-liquid mixing processes in multiphase reacting flows.

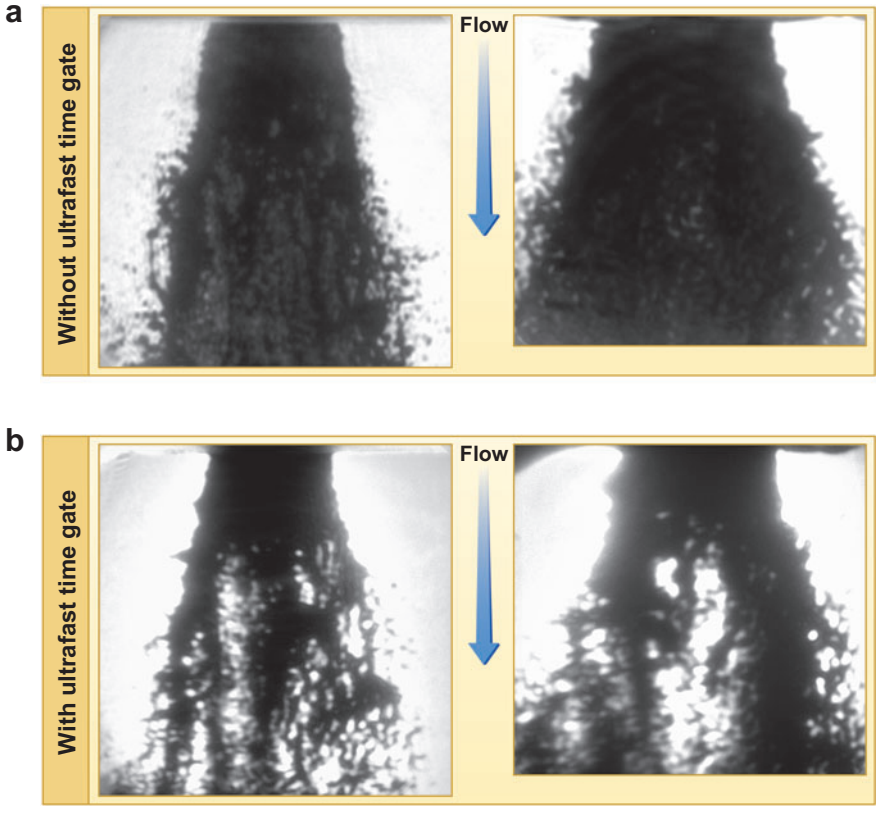

Figure 5

Sample images of rocket spray (*a*) without ultrafast time gate and (*b*) with ultrafast time gate. Flow is from top to bottom.

Advances in ultrafast laser technology have led to significant growth in the implementation of time-gated ballistic-imaging systems for visualizing hidden structures in optically dense media. A number of innovations such as two-color ballistic imaging (59) and dual-pulse ballistic imaging for velocimetry (60) have also been demonstrated recently. Future work could involve the use of three or more consecutive pulses to acquire the acceleration of interfacial regions as well as velocity within dense media. Finally, efforts are underway to use Monte Carlo simulations to predict the properties of ultrafast laser–light propagation through scattering media (61), including implementation for cases with inhomogeneously distributed scatterers.

5. ULTRAFAST COHERENT ANTI-STOKES RAMAN SCATTERING SPECTROSCOPY

CARS spectroscopy is widely used for temperature and major-species-concentration measurements in reacting flows and plasmas (1–3). Because of the phase-matching

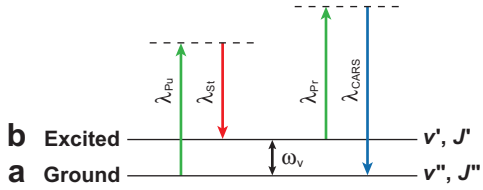

Figure 6

Energy-level diagram for coherent anti-Stokes Raman scattering signal-generation process, where *a* and *b* denote ground and excited levels of molecule, respectively, and ω_v corresponds to vibrational frequency of molecule. Here v' and J' refer to excited-state vibrational and rotational quantum number, respectively, and v'' and J'' refer to ground-state vibrational and rotational quantum number, respectively.

requirement and laser-like nature of the signal, CARS is ideally suited for reacting flows with significant background emission because one can easily isolate the CARS signal spectrally, spatially, and temporally from the flame emission. The technique also provides spatially and temporally resolved information with high accuracy.

An energy-level diagram for the CARS signal-generation process is shown in **Figure 6**. In CARS the wavelengths of the pump and Stokes beams are chosen to excite either the vibrational or rotational transitions of the molecule. We can also describe this excitation process as creating coherence in the medium with a pump-Stokes pair after which the coherence evolves according to the interaction of the molecules with the surrounding medium. When a probe beam interacts with the excited molecules, it is scattered at an anti-Stokes-shifted frequency to yield the CARS signal.

Until recently most of the CARS work in reacting flows was performed using nanosecond lasers to determine gas temperature and the concentrations of major species such as N_2, O_2, CO_2, CO, H_2, and H_2O (1, 62–65). Electronic-resonance-enhanced CARS using nanosecond lasers has also been demonstrated for determining the concentration of flame radicals such as OH, NO, and C_2H_2 (66–68). Traditional nanosecond CARS uses a narrowband (~0.001 cm^{-1}) transform-limited pump laser and a broadband (~150 cm^{-1}) Stokes laser to excite the entire rovibrational manifold of the molecule (**Figure 7*a***). For example, a narrowband laser at 532 nm and a broadband laser at ~607 nm excite the rovibrational energy levels of N_2, which is typically targeted for temperature measurements because of its abundance in air-fed reacting flows. The band head of the $v' = 1 \rightarrow v'' = 0$ transition in the ground electronic state falls at ~2330 cm^{-1}. As shown in **Figure 7*a***, only one pump-Stokes pair contributes to the excitation of the coherence for a particular transition. However, nanosecond CARS has several disadvantages that challenge its application in high-pressure, turbulent reacting flows: (*a*) interference of the nonresonant background signal with the resonant signal, which affects the accuracy and sensitivity of the measurements, especially for hydrocarbon-fueled combustion (1, 69); (*b*) the low repetition rates of the lasers used, which complicate efforts to study the temporal characteristics of turbulent flames and explore combustion instabilities; and (*c*) the need to understand the collisional environment and associated

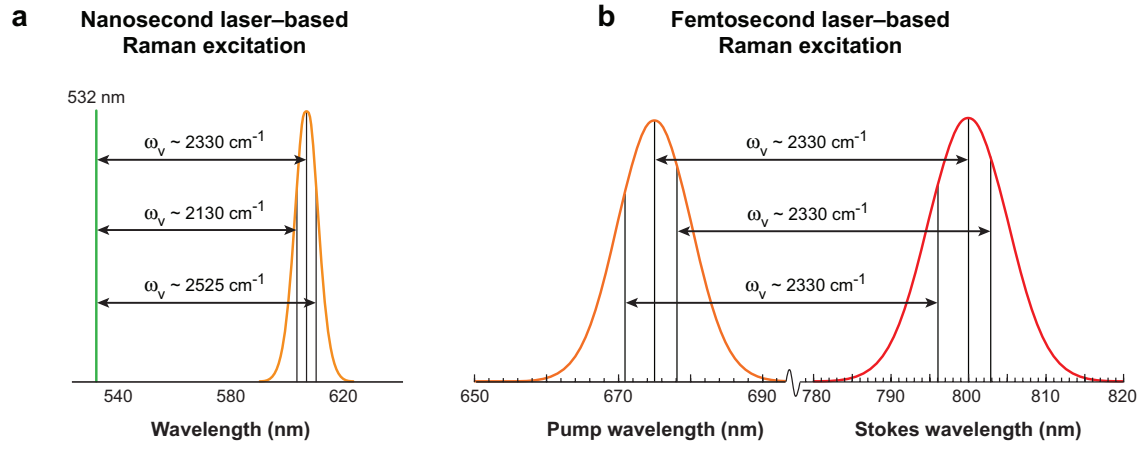

Figure 7

Raman excitation scheme for gas-phase N_2 using (*a*) nanosecond laser–based multiplex coherent anti-Stokes Raman scattering and (*b*) femtosecond pump and Stokes lasers.

dephasing and relaxation processes for quantitative interpretation of the CARS signal.

The use of ultrafast lasers to address these issues in reacting flows has been the subject of continuing research activities in the Air Force Research Laboratory's Combustion and Laser Diagnostics Research Complex at Wright-Patterson Air Force Base. In picosecond or femtosecond CARS, nonresonant background signals are observed only when all three laser beams are temporally and spatially coincident. These nonresonant interferences can be suppressed by delaying the probe beam with respect to the Raman-excitation beams. Roy et al. (69) performed picosecond multiplex CARS experiments with the probe beam delayed by ~150 ps with respect to the Raman-excitation beams. In this arrangement, the nonresonant background signal is reduced by more than three orders of magnitude, whereas the resonant signal is reduced by only a factor of three to yield a tremendous improvement in signal-to-noise ratio. However, in picosecond CARS, the quantitative interpretation of the signal still requires some knowledge of the collisional physics, and the repetition rate of the lasers used in these particular experiments is only of the order 10–20 Hz.

Femtosecond CARS spectroscopy has the potential to overcome the problems associated with nanosecond CARS for combustion applications, as evidenced by recent studies of femtosecond CARS in noncombusting environments (70–75). When two femtosecond laser pulses are used to create coherence in the medium (as in the case of CARS), the ground and excited states are coupled efficiently because of the availability of a large number of pump-Stokes pairs within the bandwidth of the laser pulses contributing to the excitation of the same coherence (**Figure 7*b***) (75). **Figure 7** shows pump-Stokes pairs for the excitation of N_2 in the ground electronic state, as mentioned above. This specific feature of femtosecond laser–based Raman excitation, along with the suppression of the nonresonant background using a delayed probe

beam, holds the potential for making the femtosecond CARS technique suitable for detecting minor species in reacting flows. Moreover, femtosecond CARS allows measurements to be made at rates of 1 kHz or greater and time-resolved CARS signals to be acquired over a time period that is short with respect to the collisional timescale, thereby eliminating the need to understand collisional broadening, line narrowing, and other dephasing and relaxation processes due to collisions.

Dantus et al. (76) eloquently describe the excitation of vibrational and rotational coherences by femtosecond lasers and the subsequent decay of these coherences either through frequency-spread dephasing or loss of alignment. Initially it was anticipated that the large bandwidths characteristic of femtosecond lasers would be problematic for molecular spectroscopy in reacting flows because of the associated lack of selectivity (broadband excitation of many transitions of one or more molecules) and relatively inefficient coupling of these spectrally broad pulses to individual transitions as compared with coupling of narrowband nanosecond pulses more closely matched to the line width of these transitions. However, the excitation process depicted in **Figure 7*b*** and recent research activities in this field have shown that the bandwidth of femtosecond lasers is actually an advantage rather than a hindrance.

In 1987 femtosecond CARS was first used to study molecular beat phenomena in liquid-phase benzene, cyclohexane, and pyridine (77); subsequently, Hayden & Chandler (78) demonstrated its application to the investigation of gas-phase molecular dynamics. Lang et al. (71) focused their work with femtosecond CARS on determining the molecular parameters and gas-phase temperature from the time-resolved oscillatory pattern of the Raman coherence following pump-Stokes excitation of H_2. They determined those parameters from the width and relative heights of the coherence recurrence peaks. The measurement of temperature from these peaks at ~320 ps, as described by Lang et al. (70), requires a detailed understanding of the collisional dephasing and relaxation physics of the probe molecule within its surrounding environment. Researchers have also used femtosecond CARS to make measurements in dense media to investigate RET processes (72), to determine the concentrations of *ortho*- and *para*-deuterium (79), and to measure single-shot temperature by probing H_2 using a chirped probe pulse (80). The technique has also been used for microscopy (81), the selective control of molecular structure (82), detection of bacterial spores (83), and investigation of the ground- and excited-state dynamics of molecules (84).

The focus of our efforts is the application of time-resolved femtosecond CARS for temperature measurements in high-temperature flames, based on the frequency-spread dephasing rate after the initial impulsive excitation of the Raman coherence in N_2 by femtosecond pump and Stokes beams. After the initial excitation, all in-phase Raman coherences excited by the nearly transform-limited laser pulses begin to oscillate out of phase with respect to each other as a result of slight differences in their frequencies. Because of the frequency differences between the neighboring transitions, the resulting coherence begins to dephase; the dephasing rate depends on temperature only and is completely insensitive to collisions (73). **Figure 8** shows time-resolved femtosecond CARS signals during the first few picoseconds after the initial impulsive excitation as a function of temperature. The coherence dephases at a faster rate with increasing temperature as a result of the contribution

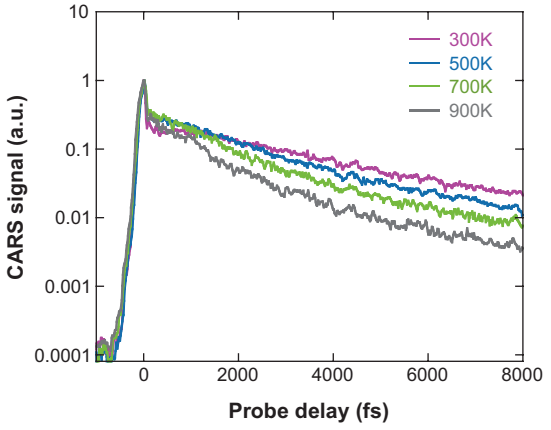

Figure 8

Temperature-dependent time-resolved femtosecond coherent anti-Stokes Raman scattering signal of N_2 (73).

from many energy levels; higher rotational and vibrational levels are populated with increasing temperature according to the Boltzmann distribution. Roy and colleagues (73–74) reported detailed theoretical and experimental results related to this concept and discussed the application of this technique in reacting flows (75). They found the estimated absolute accuracy and precision of the measurement technique to be ± 40 K and ± 50 K, respectively, over the temperature range 1500–2500 K (75). **Figure 9** illustrates the temporal evolution of time-resolved femtosecond CARS signals during the first few picoseconds after the initial excitation as a function of pressure. It is evident from **Figure 9** that the coherence dephasing rate during the first few picoseconds is insensitive to collisions. However, collisions begin to influence the dephasing rates when the pressure is increased beyond 20 bar (72). We have designed current research activities in our laboratory to address these key issues: (*a*) single-shot temperature measurements at rates of 1 kHz or greater using a spectrally chirped probe pulse, (*b*) the influence of other molecules excited by the broadband femtosecond laser pulses on measurements of temperature and species

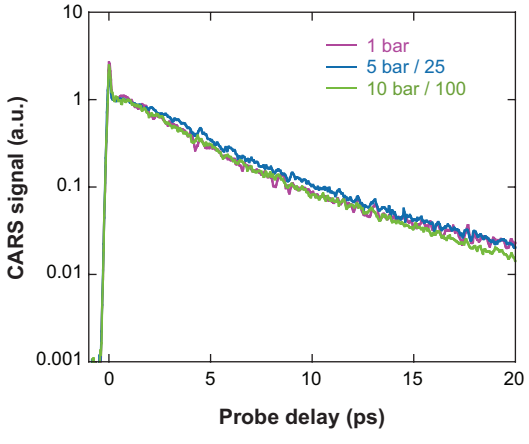

Figure 9

Pressure dependence of time-resolved N_2 femtosecond coherent anti-Stokes Raman scattering signal during first few picoseconds after impulsive excitation of the coherence.

concentrations, and (*c*) concentration measurements of minor species such as C_2H_2, C_6H_6, and other flame molecules and radicals using shaped laser pulses.

6. RESONANT AND RAMAN-INDUCED POLARIZATION SPECTROSCOPY AND WAVE MIXING

PS has emerged as a valuable spectroscopic tool for measuring the concentrations of minor species such as OH, CH, and NH in reacting flows (1–3, 85–88) and plasmas (89). PS is a nonlinear pump/probe technique in which the probe beam is linearly polarized prior to interacting with the medium of interest. PS uses either a circularly or a linearly polarized pump beam for selective pumping of the population from the ground to the excited states; in the latter case, the pump-beam polarization is rotated 45° with respect to the probe-beam polarization. Because of the anisotropy induced by the pump beam, the probe-beam polarization becomes slightly elliptical or slightly rotated while passing through the medium. As a consequence, some of the probe beam leaks through a polarization analyzer whose transmission axis is orthogonal to the original probe-beam polarization; this leakage is the PS signal. To illustrate the introduction of anisotropy by selective pumping, **Figure 10** shows an energy-level diagram of the $P_1(2)$ transition of OH. A linearly polarized pump beam couples the $\Delta M = 0$ transitions, and a right or left circularly polarized pump beam couples either the $\Delta M = +1$ or the $\Delta M = -1$ transitions, respectively.

Two distinct advantages of using ultrafast lasers for PS are (*a*) the reduction in collisional dependence and (*b*) the determination of the state-specific rotational, orientation, and alignment relaxation rates from time-resolved measurements. Roy and colleagues (86, 91) showed that when using an ultrafast laser (laser pulse width $\tau_L < \tau_C$ characteristic collision time), the collision-rate dependence of the PS signal is significantly decreased as compared with that in the long-pulse laser case

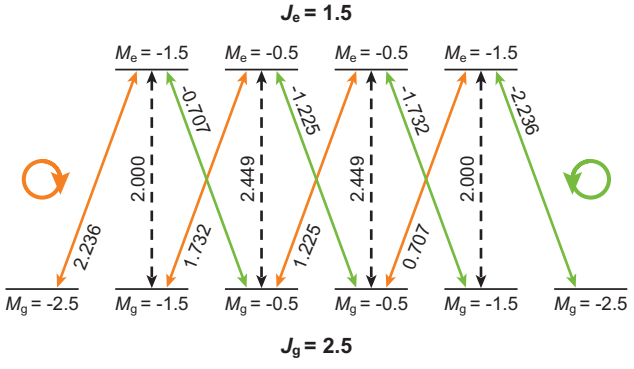

Figure 10

Energy-level diagram for Zeeman state structure of $P_1(2)$ transition. Allowed $\Delta M = 0$ transitions are indicated by dashed arrows; $\Delta M = \pm 1$ transitions are indicated by solid arrows. J and M represent rotational and projection quantum numbers, respectively. Strengths and phases of transitions are indicated by numerical value of x or z components of geometry-dependent part of the dipole matrix element (90). Figure redrawn from Reference 91.

($\tau_L > \tau_C$) for a nonsaturating pump beam. For a saturating pump beam, the picosecond PS signal is nearly independent of collisions (91).

The polarization-dependent selective pumping shown in **Figure 10** creates various types of anisotropies such as orientation and alignment in the medium with relaxation rates due to elastic (M_J changing) and inelastic RET collisions that can significantly affect the resulting PS signal and signals associated with other laser techniques that exploit laser-induced anisotropy. Orientation, which describes the net helicity or spin of the system, and alignment, which describes the spatial distribution of angular momentum, are proportional to the dipole and quadrupole moments of the angular momentum distributions, respectively (92). To illustrate the anisotropies created by the pump laser, **Figure 11** shows the population distribution in the excited Zeeman states for the $P_1(8)$ transition of OH. **Figure 11*a*** shows the oriented distribution of the excited-state population when pumped by a right circularly polarized beam, whereas **Figure 11*b*** shows the aligned distribution when pumped by a linearly polarized beam. The population distribution is shown for a time at which the 100-ps (full width at half-maximum) pump laser reaches the peak intensity of 5×10^9 W m^{-2} and was calculated using the density-matrix numerical code described by Roy et al. (91).

The use of picosecond lasers enables experimental investigation of the rates at which these anisotropies are destroyed in collisional environments. Dreizler and colleagues (93, 94) used PS and RFWM to determine the population, orientation, and alignment relaxation rates of OH in reacting flows. The RFWM technique, in which the two pump photons originate from two different pump beams, is similar to PS, in which both pump photons originate from the same pump beam. Unlike PS, the RFWM technique allows measurements of the population, orientation, and alignment relaxation rates independently through the control of polarization settings for

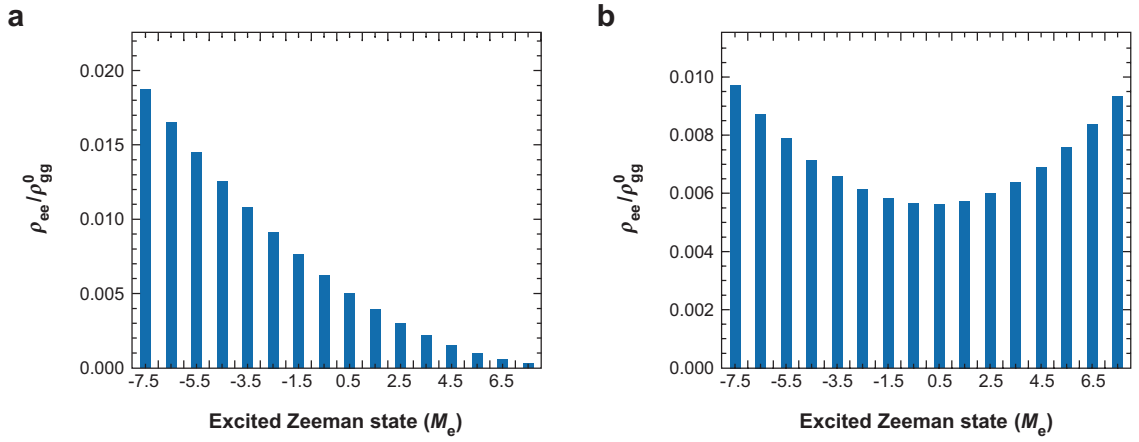

Figure 11

Population distribution in excited Zeeman states for $P_1(8)$ transition pumped by (*a*) right circularly polarized beam and (*b*) linearly polarized beam. ρ^0_{gg} is ground-state population at $t = 0$ s.

each laser beam. In an experiment in which both pump and probe beams are resonant with the same transitions, the measured relaxation rates have a contribution from both the ground and the excited states as reported by Dreizler and colleagues (93, 94). To measure the ground-state orientation and alignment relaxation rates of OH, Chen and coworkers (95) and Costen & McKendrick (96) employed two-color PS in which the pump and probe beams are coupled through an intermediate level in the ground electronic state. Chen & Settersten (97) also demonstrated two-color RFWM for determining the ground-state population, orientation, and alignment relaxation rates by varying the polarization of two pump beams and the probe beam independently. Recently, picosecond laser–based, two-color, two-photon PS was used for the detection of atomic hydrogen in an atmospheric-pressure H_2-air flame; because of its high reactivity and diffusivity, the hydrogen atom plays an important role in combustion chemical kinetics (98).

Femtosecond laser–based Raman-induced PS and degenerate four-wave mixing were used to study the ground-level RET in N_2, O_2, and CO_2 (99, 100). The broadband femtosecond lasers create a rotational wave packet by simultaneously exciting multiple rotational Raman transitions. The delayed probe beam then probes the misalignment and realignment of this rotational coherence due to elastic and inelastic collisions. These studies will have a significant impact in determining the RET rates for species relevant to reacting flows. Raman-induced degenerate four-wave mixing of H_2, in which the rotational transitions of H_2 were excited using a sub-20-fs laser pulse, has also been used to determine temperature from the relative intensities of the beat frequencies between the Stokes and anti-Stokes transitions (101).

7. CONCLUSION

Revolutionary ultrafast laser technologies are redefining the combustion-diagnostics arena. Unprecedented new measurement capabilities are emerging as researchers exploit the ultrashort pulses and high pulse-repetition rates delivered by these systems. This review highlights recent advances in ultrafast LIF, linear pump/probe techniques, time-gated ballistic imaging, ultrafast CARS, and resonant and Raman-induced PS and wave mixing. Continuing developments of ultrafast laser systems promise to provide further reductions in cost, size, and complexity with increased robustness and stability and improved user-friendliness. All these enhancements will allow the transition of ultrafast laser–based combustion diagnostics from the laboratory to the field for applications that include test-cell and shop-floor measurements, nondestructive evaluation/inspection, and onboard sensing and control.

SUMMARY POINTS

1. Detailed studies of combustion chemistry and physics are critical for the continued advancement of numerous combustion-related applications, including propulsion, power generation, industrial processing, waste incineration, and fire safety.

2. Optical combustion diagnostics are ideal tools for noninvasive characterization of reacting and nonreacting flows.
3. Although continuous-wave and nanosecond-pulsed lasers are the current sources of choice for most combustion diagnostics, emerging ultrafast (picosecond- and femtosecond-pulsed) laser technologies are driving new developments in combustion measurements.
4. Ultrashort pulses enable time-resolved measurements with unprecedented temporal resolution and freedom from collisional effects that plague measurements with nanosecond-pulsed lasers. Peak powers achievable with these pulses allow nonlinear frequency conversion, expanding the spectral coverage of these systems to new heights. Similarly, these peak powers enable nonlinear signal generation in combusting systems with lasers of moderate to low average power.
5. High pulse-repetition rates afforded by ultrafast oscillators and amplifiers provide the data-acquisition bandwidth necessary to study the temporal evolution of turbulent fluctuations and combustion instabilities. Time series and PSDs can be constructed to characterize these flame phenomena.
6. Ultrafast combustion measurements achieved to date include LIF, linear pump/probe measurements, time-gated ballistic imaging, CARS, PS, and wave mixing. In many cases the ultrafast variants described in this review enjoy numerous and significant advantages over their continuous-wave and nanosecond-pulsed analogs.
7. Continuing and future developments of ultrafast lasers hold tremendous promise for even greater spectral coverage, single-shot high-speed measurements, and application to complex real-world systems for test-cell and shop-floor measurements, nondestructive evaluation/inspection, and onboard sensing and control.

DISCLOSURE STATEMENT

The authors are not aware of any biases that might be perceived as affecting the objectivity of this review.

ACKNOWLEDGMENTS

The authors gratefully acknowledge editorial assistance provided by Ms. Marian Whitaker and continuing long-term financial support and encouragement from Dr. Julian Tishkoff, Air Force Office of Scientific Research. We also gratefully recognize a host of outstanding colleagues and collaborators with whom we have interacted over the course of the past many years. Their tremendous expertise and enthusiasm have contributed immeasurably to many of the efforts described in this review. Of particular note are the contributions of Dr. G.J. Fiechtner, Prof. G.B. King, Dr. M.A. Linne, Prof. R.P. Lucht, and Dr. T.B. Settersten.

LITERATURE CITED

1. Eckbreth AC. 1996. *Laser Diagnostics for Combustion Temperature and Species*. Amsterdam: Gordon & Breach. 596 pp. 2nd ed.
2. Kohse-Höinghaus K, Jeffries JB. 2002. *Applied Combustion Diagnostics*. New York: Taylor & Francis. 705 pp.
3. Linne MA. 2002. *Spectroscopic Measurement: An Introduction to the Fundamentals*. New York: Academic. 414 pp.
4. Laurendeau NM. 2005. *Statistical Thermodynamics: Fundamentals and Applications*. New York: Cambridge Univ. Press. 448 pp.
5. Diels J-C, Rudolph W. 2006. *Ultrashort Laser Pulse Phenomena*. New York: Academic. 680 pp. 2nd ed.
6. Rullière C, ed. 2005. *Femtosecond Laser Pulses: Principles and Experiments*. New York: Springer. 426 pp. 2nd ed.
7. Fermann ME, Galvanauskas A, Sucha G. 2003. *Ultrafast Lasers: Technology and Applications*. New York: Marcel Dekker. 784 pp.
8. Hobbs PCD. 2000. *Building Electro-Optical Systems: Making It All Work*. New York: Wiley & Sons. 727 pp.
9. Hartlieb AT, Markus D, Kreutner W, Kohse-Höinghaus K. 1997. Measurement of vibrational energy transfer of OH ($A^2\Sigma^+$, $v' = 1 \rightarrow 0$) in low pressure flames. *Appl. Phys. B* 65:81–91
10. Beaud P, Radi PP, Franzke D, Frey H-M, Mischler B, et al. 1998. Picosecond investigation of the collisional deactivation of OH $A^2\Sigma^+$ ($v' = 1, N' = 4, 12$) in an atmospheric-pressure flame. *Appl. Opt.* 37:3354–67
11. Nielsen T, Bormann F, Burrows M, Andresen P. 1997. Picosecond laser-induced fluorescence measurement of rotational energy transfer of OH $A^2\Sigma^+$ ($v' = 2$) in atmospheric pressure flames. *Appl. Opt.* 36:7960–69
12. Agrup S, Ossler F, Aldén M. 1995. Measurements of collisional quenching of hydrogen atoms in an atmospheric-pressure hydrogen oxygen flame by picosecond laser-induced fluorescence. *Appl. Phys. B* 61:479–87
13. Settersten TB, Patterson BD, Kronemayer H, Sick V, Schulz C, Daily JW. 2006. Branching ratios for quenching of nitric oxide $A^2\Sigma^+$ ($v' = 0$) to $X^2\Pi$ ($v'' = 0$). *Phys. Chem. Chem. Phys.* 8:5328–38
14. Brockhinke A, Kreutner W, Rahmann U, Kohse-Höinghaus K, Settersten TB, Linne MA. 1999. Time-, wavelength-, and polarization-resolved measurements of OH $A^2\Sigma^+$ picosecond laser-induced fluorescence in atmospheric-pressure flames. *Appl. Phys. B* 69:477–85
15. Agrup S, Aldén M. 1994. Two-photon laser-induced fluorescence and stimulated emission measurements from oxygen atoms in a hydrogen/oxygen flame with picosecond resolution. *Opt. Commun.* 113:315–23
16. Frank JH, Chen X, Patterson BD, Settersten TB. 2004. Comparison of nanosecond and picosecond excitation for two-photon laser-induced fluorescence imaging of atomic oxygen in flames. *Appl. Opt.* 43:2588–97
17. Settersten TB, Dreizler A, Farrow RL. 2002. Temperature- and species-dependent quenching of CO *B* probed by two-photon laser-induced fluorescence using a picosecond laser. *J. Chem. Phys.* 117:3173–79

18. Settersten TB, Patterson BD, Gray JA. 2006. Temperature- and species-dependent quenching of NO $A^2\Sigma^+$ ($v' = 0$) probed by two-photon laser-induced fluorescence using a picosecond laser. *J. Chem. Phys.* 124:234308
19. Brockhinke A, Bülter A, Rolon JC, Kohse-Hoinghaus K. 2001. ps-LIF measurements of minor species concentration in a counter diffusion flame interactive with a vortex. *Appl. Phys. B* 72:491–96
20. Ossler F, Metz T, Martinsson L, Aldén M. 1998. Two-dimensional visualization of fluorescence lifetimes by use of a picosecond laser and a streak camera. *Appl. Opt.* 37:2303–14
21. Klassen MS, Thompson BD, Reichardt TA, King GB, Laurendeau NM. 1994. Flame concentration measurements using picosecond time-resolved laser-induced fluorescence. *Combust. Sci. Technol.* 97:391–403
22. Pack SD, Renfro MW, King GB, Laurendeau NM. 1999. Laser-induced fluorescence triple-integration method applied to hydroxyl concentration and fluorescence lifetime measurements. *Combust. Sci. Technol.* 140:405–25
23. Renfro MW, King GB, Laurendeau NM. 2000. Scalar time-series measurements in turbulent $CH_4/H_2/N_2$ nonpremixed flames: CH. *Combust. Flame* 122:139–50
24. Renfro MW, King GB, Laurendeau NM. 1999. Quantitative hydroxyl concentration time-series measurements in turbulent nonpremixed flames. *Appl. Opt.* 38:4596–608
25. Meyer TR, King GB, Gluesenkamp M, Gord JR. 2007. Simultaneous high-speed measurement of temperature and lifetime-corrected OH laser-induced fluorescence in unsteady flames. *Opt. Lett.* 32:2221–23
26. Elzinga PA, Lytle FE, Jiang Y, King GB, Laurendeau NM. 1987. Pump/probe spectroscopy by asynchronous optical sampling. *Appl. Spectrosc.* 41:2–4
27. Elzinga PA, Kneisler RJ, Lytle FE, Jiang Y, King GB, Laurendeau NM. 1987. Pump/probe method for fast analysis of visible spectral signatures utilizing asynchronous optical sampling. *Appl. Opt.* 26:4303–9
28. Kneisler RJ, Lytle FE, Fiechtner GJ, Jiang Y, King GB, Laurendeau NM. 1989. Asynchronous optical sampling: a new combustion diagnostic for potential use in turbulent, high-pressure flames. *Opt. Lett.* 14:260–62
29. Fiechtner GJ, King GB, Laurendeau NM, Lytle FE. 1992. Measurements of atomic sodium in flames by asynchronous optical sampling: theory and experiment. *Appl. Opt.* 31:2849–64
30. Fiechtner GJ. 1992. *Quantitative concentration measurements in atmospheric-pressure flames by picosecond pump/probe absorption spectroscopy*. PhD thesis. Purdue Univ.
31. Fiechtner GJ, King GB, Laurendeau NM. 1995. Quantitative concentration measurements of atomic sodium in an atmospheric hydrocarbon flame with asynchronous optical sampling. *Appl. Opt.* 34:1117–26
32. Fiechtner GJ, King GB, Laurendeau NM. 1995. Rate-equation model for quantitative concentration measurements in flames by picosecond pump-probe absorption spectroscopy. *Appl. Opt.* 34:1108–16

33. Fiechtner GJ, Linne MA. 1994. Absolute concentrations of potassium by picosecond pump/probe absorption in fluctuating, atmospheric pressure flame. *Combust. Sci. Technol.* 100:11–27
34. Settersten TB. 1999. *Picosecond pump/probe diagnostics for combustion*. PhD thesis. Colo. School of Mines
35. Settersten TB, Linne MA. 2002. Picosecond pump-probe absorption spectroscopy in gases: models and experimental validation. *Appl. Opt.* 41:2869–78
36. Settersten T, Linne M, Gord J, Fiechtner G. 1999. Density matrix and rate equation analyses for picosecond pump/probe combustion diagnostics. *AIAA J.* 37:723–31
37. Settersten TB, Linne MA. 2002. Modeling pulsed excitation for gas-phase laser diagnostics. *J. Opt. Soc. Am. B* 19:954–64
38. Linne MA, Morse DC, Skilowitz JL, Fiechtner GJ, Gord JR. 1995. Two-dimensional pump-probe imaging in reacting flows. *Opt. Lett.* 20:2414–16
39. Mittleman D, ed. 2003. *Sensing with Terahertz Radiation*. New York: Springer. 337 pp.
40. Cheville RA, Grischkowsky D. 1995. Far-infrared, terahertz time-domain spectroscopy of flames. *Opt. Lett.* 20:1646–48
41. Cheville RA, Grischkowsky D. 1998. Observation of pure rotational absorption spectra in the ν_2 band of hot H_2O in flames. *Opt. Lett.* 23:531–33
42. Brown MS, Fiechtner GJ, Rudd JV, Zimdars DA, Warmuth M, Gord JR. 2006. Water-vapor detection using asynchronous THz sampling. *Appl. Spectrosc.* 60:261–65
43. Schmitt JM, Knüttel A, Yadlowsky M. 1994. Confocal microscopy in turbid media. *J. Opt. Soc. Am. A* 11:2226–35
44. Kempe M, Genack AZ, Rudolph W, Dorn P. 1997. Ballistic and diffuse light detection in confocal and heterodyne imaging systems. *J. Opt. Soc. Am. A* 14:216–23
45. Demos SG, Alfano RR. 1996. Temporal gating in highly scattering media by the degree of optical polarization. *Opt. Lett.* 21:161–63
46. Mujumdar S, Ramachandran H. 2004. Imaging through turbid media using polarization modulation: dependence on scattering anisotropy. *Opt. Commun.* 241:1–9
47. Fujimoto JG, De Silvestri S, Ippen EP, Puliafito CA, Margolis R, Oseroff A. 1986. Femtosecond optical ranging in biological systems. *Opt. Lett.* 11:150–52
48. Yoo KM, Xing Q, Alfano RR. 1991. Imaging objects hidden in highly scattering media using femtosecond second-harmonic-generation cross-correlation time gating. *Opt. Lett.* 16:1019–21
49. Bordenave E, Abraham E, Jonusauskas G, Oberlé J, Rullière C. 2002. Longitudinal imaging in biological tissues with a single laser shot correlation system. *Opt. Exp.* 10:35–40
50. Kippelen B, Marder SR, Hendrickx E, Maldonado JL, Guillemet G, et al. 1998. Infrared photorefractive polymers and their applications for imaging. *Science* 279:54–57
51. Duguay MA, Mattick AT. 1971. Ultrahigh speed photography of picoseond light pulses and echoes. *Appl. Opt.* 10:2162–70

52. Sala K, Richardson MC. 1975. Optical Kerr effect induced by ultrashort pulses. *Phys. Rev. A* 12:1036–47
53. Ho PP, Alfano RR. 1979. Optical Kerr effect in liquids. *Phys. Rev. A* 20:2170–87
54. Wang L, Ho PP, Liu C, Zhang G, Alfano RR. 1991. Ballistic 2-D imaging through scattering walls using an ultrafast optical Kerr gate. *Science* 253:769–71
55. Galland PA, Liang X, Wang L, Breisacher K, Liou L, et al. 1995. Time-resolved optical imaging of jet sprays and droplets in highly scattering medium. *Proc. Am. Soc. Mech. Eng.* HTD-321:585–88
56. Paciaroni M, Linne M. 2004. Single-shot, two-dimensional ballistic imaging through scattering media. *Appl. Opt.* 43:5100–9
57. Paciaroni M, Linne M, Hall T, Delplanque J-P, Parker T. 2006. Single-shot two-dimensional ballistic imaging of the liquid core in an atomizing spray. *At. Sprays* 16:51–70
58. Linne M, Paciaroni M, Hall T, Parker T. 2006. Ballistic imaging of the near field in a diesel spray. *Exp. Fluids* 40:836–46
59. Linne MA, Paciaroni M, Gord JR, Meyer TR. 2005. Ballistic imaging of the liquid core for a steady jet in crossflow. *Appl. Opt.* 44:6627–34
60. Sedarsky DL, Paciaroni ME, Linne MA, Gord JR, Meyer TR. 2006. Velocity imaging for the liquid-gas interface in the near field of an atomizing spray: proof of concept. *Opt. Lett.* 31:906–8
61. Wang X, Wang LV, Sun C-W, Yang C-C. 2003. Polarized light propagation through scattering media: time-resolved Monte Carlo simulations and experiments. *J. Biomed. Opt.* 8:608–17
62. Roy S, Meyer TR, Brown MS, Velur VN, Lucht RP, Gord JR. 2003. Triple-pump coherent anti-Stokes Raman scattering (CARS): temperature and multiple-species concentration measurements in reacting flows. *Opt. Commun.* 224:131–37
63. Meyer TR, Roy S, Lucht RP, Gord JR. 2005. Dual-pump dual-broadband CARS for exhaust-gas temperature and CO_2-O_2-N_2 mole-fraction measurements in model gas-turbine combustors. *Combust. Flame* 142:52–61
64. Hall RJ, Shirley JA. 1983. Coherent anti-Stokes Raman spectroscopy of water vapor for combustion diagnostics. *Appl. Spectrosc.* 37:196–202
65. Rahn LA, Zych LJ, Mattern PL. 1979. Background-free CARS studies of carbon monoxide in a flame. *Opt. Commun.* 30:249–52
66. Attal-Trétout B, Schmidt SC, Crété E, Dumas P, Taran JP. 1990. Resonance CARS of OH in high-pressure flames. *J. Quant. Spectrosc. Radiat. Transf.* 43:351–64
67. Roy S, Kulatilaka WD, Naik SV, Laurendeau NM, Lucht RP, Gord JR. 2006. Effects of quenching on electronic-resonance-enhanced coherent anti-Stokes Raman scattering of nitric oxide. *Appl. Phys. Lett.* 89:104105
68. Chai N, Naik SV, Kulatilaka WD, Laurendeau NM, Lucht RP, et al. 2007. Detection of acetylene by electronic resonance-enhanced coherent anti-Stokes Raman scattering. *Appl. Phys. B* 87:731–37
69. Roy S, Meyer TR, Gord JR. 2005. Time-resolved dynamics of resonant and nonresonant broadband picosecond coherent anti-Stokes Raman scattering signals. *Appl. Phys. Lett.* 87:264103

70. Lang T, Motzkus M, Frey HM, Beaud P. 2001. High resolution femtosecond coherent anti-Stokes Raman scattering: determination of rotational constants, molecular anharmonicity, collisional line shifts, and temperature. *J. Chem. Phys.* 115:5418–26
71. Lang T, Kompa KL, Motzkus M. 1999. Femtosecond CARS on H_2. *Chem. Phys. Lett.* 310:65–72
72. Knopp G, Beaud P, Radi P, Tulej M, Bougie B, et al. 2002. Pressure-dependent N_2 Q-branch fs-CARS measurements. *J. Raman Spectrosc.* 33:861–65
73. Lucht RP, Roy S, Meyer TR, Gord JR. 2006. Femtosecond coherent anti-Stokes Raman scattering measurement of gas temperatures from frequency-spread dephasing of the Raman coherence. *Appl. Phys. Lett.* 89:251112
74. Lucht RP, Kinnius PJ, Roy S, Gord JR. 2007. Theory of femtosecond coherent anti-Stokes Raman scattering spectroscopy of gas-phase resonant transitions. *J. Chem. Phys.* 127:044316
75. Roy S, Kinnius PJ, Lucht RP, Gord JR. 2008. Temperature measurements in reacting flows by time-resolved femtosecond coherent anti-Stokes Raman scattering (fs-CARS) spectroscopy. *Opt. Commun.* 281:319–25
76. Dantus M, Bowman RM, Zewail AH. 1990. Femtosecond laser observations of molecular vibration and rotation. *Nature* 343:737–39
77. Leonhardt R, Holzapfel W, Zinth W, Kaiser W. 1987. Terahertz quantum beats in molecular liquids. *Chem. Phys. Lett.* 133:373–77
78. Hayden CC, Chandler DW. 1995. Femtosecond time-resolved studies of coherent vibrational Raman scattering in large gas-phase molecules. *J. Chem. Phys.* 103:10465–72
79. Knopp G, Kirch K, Beaud P, Mishima K, Spitzer H, et al. 2003. Determination of the ortho-/para deuterium concentration ratio with femtosecond CARS. *J. Raman Spectrosc.* 34:989–93
80. Lang T, Motzkus M. 2002. Single-shot femtosecond coherent anti-Stokes Raman-scattering thermometry. *J. Opt. Soc. Am. B* 19:340–44
81. Cheng JX, Xie XS. 2004. Coherent anti-Stokes Raman scattering microscopy: theory, instrumentation, and applications. *J. Phys. Chem. B* 108:827–40
82. Weiner AM, Leaird DE, Wiederrecht GP, Nelson KA. 1990. Femtosecond pulse sequences used for optical manipulation of molecular motion. *Science* 247:1317–19
83. Scully MO, Kattawar GW, Lucht RP, Opatrný T, Pilloff H, et al. 2002. FAST CARS: engineering a laser spectroscopic technique for rapid identification of bacterial spores. *Proc. Nat. Acad. Sci. USA* 99:10994–1001
84. Schmitt M, Knopp G, Materny A, Kiefer W. 1998. The application of femtosecond time-resolved coherent anti-Stokes Raman scattering for the investigation of ground and excited state molecular dynamics of molecules in the gas phase. *J. Phys. Chem. A* 102:4059–65
85. Demtröder W. 2002. *Laser Spectroscopy*. New York: Springer. 987 pp. 3rd ed.
86. Reichardt TA, Teodoro FD, Farrow RL, Roy S, Lucht RP. 2000. Collisional dependence of polarization spectroscopy with a picosecond laser. *J. Chem. Phys.* 113:2263–69

87. Keifer J, Li Z, Zetterberg J, Linvin M, Aldén M. 2007. Simultaneous laser-induced fluorescence and sub-Doppler polarization spectroscopy of the CH radical. *Opt. Commun.* 270:347–52
88. Tobai J, Dreier T. 1999. Measurement of relaxation times of NH in atmospheric pressure flames using picosecond pump-probe degenerate four-wave mixing. *J. Mol. Struct.* 480–481:307–10
89. Danzmann K, Grützmacher K, Wende B. 1986. Doppler-free two-photon polarization-spectroscopic measurement of the Stark-broadened profile of the hydrogen La line in a dense plasma. *Phys. Rev. Lett.* 57:2151–53
90. Sargent M III, Scully MO, Lamb WE Jr. 1974. *Laser Physics*. Boulder, CO: Westview Press. 464 pp.
91. Roy S, Lucht RP, Reichardt TA. 2002. Polarization spectroscopy using short-pulse lasers: theoretical analysis. *J. Chem. Phys.* 116:571–80
92. Zare RN. 1988. *Angular Momentum: Understanding Spatial Aspects in Chemistry and Physics*. New York: Wiley & Sons. 368 pp.
93. Dreizler A, Taddy R, Suvernev AA, Himmelhaus M, Dreier T, Foggi P. 1995. Measurement of orientational relaxation times of OH in a flame using picosecond time-resolved polarization spectroscopy. *Chem. Phys. Lett.* 240:315–23
94. Tadday R, Dreizler A, Suvernev AA, Dreier T. 1997. Measurement of orientational relaxation times of OH ($A^2\Sigma$–$X^2\Pi$) transitions in atmospheric pressure flames using picosecond time-resolved nonlinear spectroscopy. *J. Mol. Struct.* 410–411:85–88
95. Chen X, Patterson BD, Settersten TB. 2004. Time-domain investigation of OH ground-state energy transfer using picosecond two-color polarization spectroscopy. *Chem. Phys. Lett.* 388:358–62
96. Costen ML, McKendrick KG. 2005. Orientation and alignment moments in two-color polarization spectroscopy. *J. Chem. Phys.* 122:164309
97. Chen X, Settersten TB. 2007. Investigation of OH $X^2\Pi$ collisional kinetics in a flame using picosecond two-color resonant four-wave-mixing spectroscopy. *Appl. Opt.* 46:3911–20
98. Kulatilaka WD, Lucht RP, Roy S, Gord JR, Settersten TB. 2007. Detection of atomic hydrogen in flames using picosecond two-color two-photon-resonant six-wave-mixing spectroscopy. *Appl. Opt.* 46:3921–27
99. Morgan M, Price W, Hunziker L, Ludowise P, Blackwell M, Chen Y. 1993. Femtosecond Raman-induced polarization spectroscopy studies of rotational coherence in O_2, N_2 and CO_2. *Chem. Phys. Lett.* 209:1–9
100. Frey HM, Beaud P, Gerber T, Mischler B, Radi PP, Tzannis AP. 1999. Femtosecond nonresonant degenerate four-wave mixing at atmospheric pressure and in a free jet. *Appl. Phys. B* 68:735–39
101. Hornung T, Skenderovic H, Kompa KL, Motzkus M. 2004. Prospect of temperature determination using degenerate four-wave mixing with sub-20 fs pulses. *J. Raman Spectrosc.* 35:934–38